9-1-2009

Casimir chemistry

D. P. Sheehan
University of San Diego, dsheehan@sandiego.edu

Casimir chemistry

D. P. Sheehan[a)]
Department of Physics, University of San Diego, San Diego, California 92110, USA

(Received 6 April 2009; accepted 26 June 2009; published online 14 September 2009)

It is shown that, at the nanoscale, the Casimir effect can be used to mechanically *tune* critical aspects of chemical reactions (e.g., energies, equilibrium constants, activation energies, transition states, reaction rates) by varying the spacing and composition of reaction vessel boundaries. This suggests new modalities for catalysts, nanoscale chemical manufacturing, chemical-mechanical engines, and biochemical processes in organisms. © *2009 American Institute of Physics*.
[doi:10.1063/1.3224158]

I. INTRODUCTION

Electromagnetic zero point fluctuations[1–3] are integral to a broad spectrum of phenomena, including the Casimir effect,[4] spontaneous emission of radiation,[5] the Davies–Unruh effect,[6,7] the Lamb shift,[8,9] the Casimir–Polder effect,[10] van der Waals forces,[11–13] the anomalous magnetic moment of the electron,[14] adhesion (stiction), friction, wetting, gas-liquid condensation, interactions of colloids and aerosols, cellular biology, laser linewidths, and the stability of atoms.[15]

The Casimir effect, originally investigated in the context of colloids,[4] has been studied extensively both theoretically and experimentally, and now finds wide application across chemistry, physics, engineering, and biology.[3,13] Until now, its connections with atomic and molecular systems have been confined primarily to physical and optical phenomena, such as the Casimir–Polder effect,[10] latent heats of vaporization,[16] surface tension,[17] and atomic spectroscopy.[18] This article examines how the Casimir effect can bear on chemical phenomena at nanometer distance scales. Specifically, it is shown that, by suitably engineering and manipulating the boundaries of micro- or nanoscopic reaction vessels, the Casimir effect can shift chemical reaction energies and equilibria and alter activation energies, transition states, and reaction rates. As a result, Casimir processes could hold applications for micro- and nanoscopic chemical reactors, catalysts, and chemical-mechanical motors, as well as for the machinery of living cells.

The remainder of this paper is organized as follows. In Sec. II relevant fundamentals of the Casimir effect are summarized, followed in Sec. III by a thought experiment demonstrating the Casimir chemical effect. In Sec. IV several potential applications are explored; directions for future research are suggested in Sec. V.

It is maintained throughout that zero point operations are *conservative*; that is, no cyclic process can be used to extract net energy from the zero point field. This is in contrast to a minority but vocal viewpoint that posits that net energy *can* be extracted cyclically from zero point field.[19] While experimental and theoretical evidence abounds for the existence of zero point energy, there is no convincing evidence for its nonconservative extraction.

II. THEORY

The Casimir effect is the pressure (positive or negative) exerted on surfaces due to the exclusion of zero point modes between them. (Alternatively, it can be explained in terms of van der Waals forces, as correlated electric and magnetic field fluctuations in the media of the affected structures. Here we adopt the zero point model.) In its original formulation, the Casimir effect referred to interactions between perfectly electrically conducting parallel plates;[4] however, it was soon generalized to interactions between arbitrary dielectric surfaces.[20] This so-called Lifshitz formalism, with its various technical refinements,[21] is generally considered valid and has been verified by numerous experiments.[22–25]

The full Lifshitz formalism is analytically intractable for all but the most idealized cases, e.g., parallel plates, spheres, or cylinders. For this study, which seeks merely to illuminate new facets of the Casimir effect, it will suffice to use approximate formulas that capture its essential features. The discussion will be restricted to parallel plate geometry, although interesting effects can arise in more complex geometries (e.g., spherical, cylindrical, corrugated surfaces). For details, the reader is directed to more complete treatments.[3,13]

A. Parallel plate Casimir effect

Consider two thick (semi-infinite), parallel dielectric plates[26] composed of media α and β [Fig. 1(a)], narrowly separated by distance z in a medium m. (Here the medium will be exclusively vacuum.) To first order, the Casimir interaction energy per unit area is given by[13]

$$E_{\beta m\alpha} = -\frac{H_{\beta m\alpha}(z)}{12\pi z^2}, \tag{1}$$

where $H_{\beta m\alpha}$ is the Hamaker coefficient pertinent to materials β, α, and m. Although H is a variable function of z, it is usually given in terms of its zero-separation value. As evident in Table I, H can vary over roughly two orders of mag-

a)Electronic mail: dsheehan@sandiego.edu. Telephone: 619-260-4095.

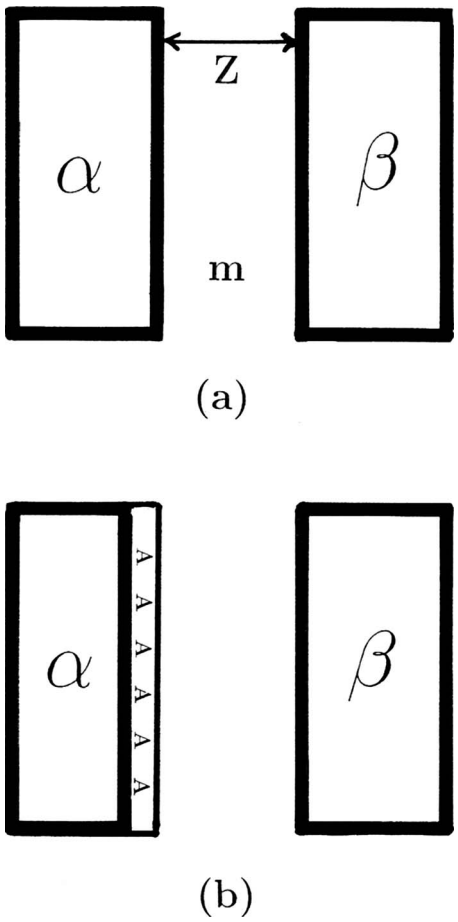

FIG. 1. Semi-infinite dielectric slabs α and β separated by medium m. α-plate is stationary and β-plate is movable in z direction. (a) Bare dielectric plates and (b) α-plate coated with thin layer of species A.

nitude depending on the interacting substances and the intervening dielectric m. It can be calculated fairly precisely from experimental values of the media's frequency-dependent dielectric response functions.

For the case of semi-infinite parallel plates at nonzero temperature, the Hamaker coefficient is given by [Fig. 1(a)][27]

$$H_{\beta m\alpha} \simeq \frac{3}{2} kT \sum_{n=0}^{\infty}{}' \Delta_{\alpha m} \Delta_{\beta m} R_n(z). \tag{2}$$

Here the subscripts $\beta m\alpha$, αm, βm refer to the interfaces between media α, β, and m, kT is the thermal energy, and $\Delta_{\alpha m,\beta m}$ are defined as

$$\Delta_{\alpha m} \equiv \frac{\epsilon_\alpha - \epsilon_m}{\epsilon_\alpha + \epsilon_m}, \quad \Delta_{\beta m} \equiv \frac{\epsilon_\beta - \epsilon_m}{\epsilon_\beta + \epsilon_m}. \tag{3}$$

Here ϵ_i are the frequency-dependent dielectric susceptibilities of α, β, and m; for vacuum $\epsilon_m \equiv \epsilon_{\text{vacuum}} = 1$. In the computation of H, the sum $\Sigma_{n=0}^{\infty}$ extends over the Matsubara sampling frequencies, $f_n = (kT/h)n$ $(n = 1, 2, 3\ldots$; h is Planck's constant), a set of discrete (positive) imaginary frequencies that span the frequency range appropriate to the Casimir effect, in increments of the thermal energy kT. For most applications, pertinent frequencies range from the IR into the deep UV.

TABLE I. Select Hamaker coefficients H (in zJ) for near-zero plate separation across vacuum and water (Ref. 13).

Substance	Vacuum	Water
Ag	200–500	100–400
Cu	400	300
Diamond (IIa)	296	138
TiO_2 (rutile)	181	60
SiO_2 (quartz)	66	1.6
PMMA	58	1.5
Polystyrene	79	13

In Eq. (2), $R_n(z)$ is a relativistic retardation correction factor that accounts for the finite speed of light and its effect on the correlation between field fluctuations in the plates' media. If a mode period is less than or equal to the light travel time in the gap, then $R_n \simeq 1$; it falls to zero as the light travel time becomes large compared with the mode period. For a vacuum gap z and for mode wavelength λ, one has $R_n(z \ll \lambda) \simeq 1$, $R_n(z \sim \lambda) \simeq 1/2$, and $R_n(z \gg \lambda) \to 0$. In effect, $R_n(z)$ offsets the dominance of short wavelength modes arising from the Matsubara summation.

As rough rules of thumb concerning the Casimir effect: (i) at a given plate separation the dominantly contributing modes have wavelengths less than or comparable to the gap distance; (ii) a mode and its effects penetrate roughly one wavelength into a medium; (iii) Casimir forces *see* into a medium roughly the distance of separation between the objects (or in the case of good conductors, the electronic screening distance); and (iv) the more disparate the values of ϵ between interacting media, the more negative the Casimir energy. Our analysis will concentrate on small distances of a few nanometers or less, so the most relevant frequencies will be in the UV portion of the spectrum.

Combining Eqs. (1) and (2), the Casimir interaction energy between two parallel plates composed of materials α and β and separated by a distance z in medium m [Fig. 1(a)] can be written as

$$E_{\alpha m\beta} \simeq -\frac{kT}{8\pi z^2} \sum_{n=0}^{\infty}{}' \Delta_{\alpha m} \Delta_{\beta m} R_n(z). \tag{4}$$

For our interests, a slightly more complicated system is called for, one having an additional thin layer of species A on plate α (thickness t_A), as portrayed in Fig. 1(b). In this case, the Casimir interaction energy is the sum of two parts, corresponding to two pairs of interacting interfaces,

$$E_{\beta mA\alpha}(z; t_A) = E_{\beta m/Am} + E_{\beta m/\alpha A} = -\frac{H_{\beta m/Am}(z)}{12\pi z^2} - \frac{H_{\beta m/\alpha A}(z + t_A)}{12\pi (z + t_A)^2}. \tag{5}$$

Here,

$$H_{\beta m/Am}(z) \simeq \frac{3}{2} kT \sum_{n=0}^{\infty}{}' \Delta_{\beta m} \Delta_{Am} R_n(z) \tag{6}$$

and

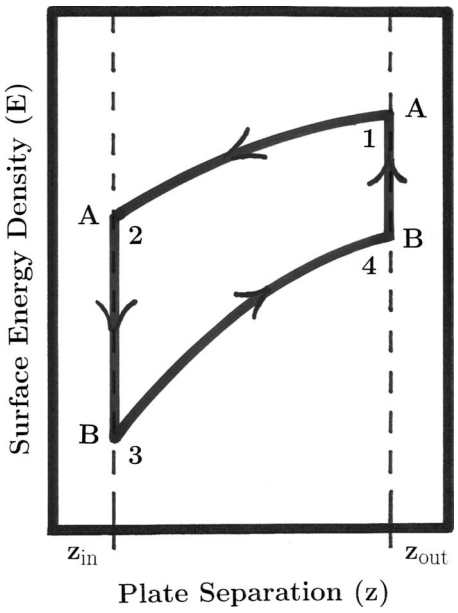

FIG. 2. Casimir surface energy density vs plate separation, pertinent to plates in Fig. 1(b) for reaction A⇌B. Chemical reaction energy varies with plate separation due to Casimir interaction.

$$H_{\beta m/\alpha A}(z+t_A) \simeq \frac{3}{2}kT\sum_{n=0}^{\infty}{}'\Delta_{\beta m}\Delta_{\alpha A}R_n(z+t_A), \tag{7}$$

where Δs are defined similarly as in Eq. (3). The first term on the right-hand side of Eq. (5) gives the interaction energy of β with respect to A, while the second term gives it for β with respect to α. As z becomes comparable to and less than t_A, the first term on the right-hand side of Eq. (5) increasingly dominates, retrieving Eq. (4) in the limit $t_A \gg z$. The first term in Eq. (5), which gives the interaction energy of species A with the β-plate, will be the primary contributor to the Casimir chemical effect.

The analysis thus far assumes a z^{-2} dependence for the surface energy density, but the actual situation is less clear cut.[3,13] Indeed, for $z \leqslant 2$ nm the energy density can be taken to vary as $E \sim z^{-2}$; however as z approaches 50 nm, the z-dependence changes to $E \sim z^{-3}$ and remains so out to about 10^3 nm, after which it returns to $E \sim z^{-2}$. Unless otherwise noted, this discussion focuses on $z \leqslant 2$ nm, so Eqs. (1)–(5) hold well.

III. CASIMIR CHEMICAL EFFECT

We now introduce the central result of this study: the effect of zero point fluctuations (Casimir effect) on chemical reaction energies. This can be demonstrated through a simple chemical-mechanical cycle (Fig. 2), based on the system shown in Fig. 1(b).

Consider two parallel plates, whose lateral dimensions are large compared with their initial separation in vacuum, z_{out}. Let z_{out} be sufficiently large that the Casimir interaction between the two plates is negligible ($z_{out} > 10^3$ nm). The left-hand plate (material α) is stationary, while the right-hand plate (material β) is inwardly movable from z_{out} to z_{in}. The stationary α plate is thinly coated with substance A (thickness t_A), which can convert into substance B. The reaction (A⇌B) might involve, for example, chemical or hydrogen bonds, changes in material phase, or molecular conformational rearrangements. (A⇌B can also be shorthand for more complex reactions involving multiple species.) To begin, it is presumed that surfaces α and β are chemically and catalytically inert with respect to A and B, aside from unavoidable physisorption due to van der Waals interactions. In fact, the A-layer need not even be in contact with α; it can be freestanding.

For the cycle depicted in Fig. 2, the abscissa corresponds to the plate separation (z) and the ordinate to the surface energy density (J/m^2) of the entire two-plate system including substance A. The cycle is performed quasistatically and is taken to be thermodynamically reversible. In the initial state of the cycle, the movable plate is out, coated with substance A. This four-step cycle, consisting of two mechanical steps involving Casimir energy and two chemical steps involving chemical energy, proceeds as follows.

Step $1 \rightarrow 2$: Plate β is moved from z_{out} inward to z_{in}, releasing mechanical Casimir energy via the Casimir force, $E_1 = E_{\beta mA\alpha}(z_{in}; t_A)$, as defined in Eq. (5).

Step $2 \rightarrow 3$: Substance A is quasistatically transformed into substance B, releasing chemical energy $E_2 = E_{chem}$ $(A \rightarrow B; z_{in})$. (By caveat, this reaction is taken to be exothermic.)

Step $3 \rightarrow 4$: Plate β is returned to z_{out}, requiring the input of mechanical work against the Casimir force, $E_3 = -E_{\beta mB\alpha}(z_{in}; t_A)$.

Step $4 \rightarrow 1$: Substance B is quasistatically transformed back into A, requiring chemical energy $E_4 = E_{chem}$ $(B \rightarrow A; z_{out})$. This step completes the cycle.

Since the cycle is closed and since energy is a state function, the net energy change around the cycle is zero; (i.e., $\oint dE = 0 = E_1 + E_2 + E_3 + E_4$). Now, because the Hamaker coefficients for A and B are distinct with respect to β and α, so too must be their interaction energies; i.e., $E_1 \neq E_3$. If this is so, then the conservation of energy constraint requires that $E_2 \neq E_4$. In other words, if the Casimir interaction energies are different for substances A and B, the chemical energy for the reaction A⇌B must depend on the relative position and composition of the reaction plates.

At first sight, this conclusion is jarring. Normally, the energy of a chemical reaction is considered independent of the geometry of its containment vessel, e.g., whether the reaction is carried out in a test tube or in an Erlenmeyer flask. While this is generally true at macroscopic scales, this cycle demonstrates otherwise for the nanoscale; indeed, for separations less than about 100 nm, zero point modes (Casimir effect) can be decisive. This is the principal result of this study; the remainder will explore its implications.

A. Chemical implications

The primary result can be extended to related cases. In Fig. 2, the reaction energy ($\Delta E_{chem} \equiv |E_A - E_B|$) is larger at z_{out} than at z_{in}, owing to the stronger Casimir interaction of A with β than for B with β. Figure 3(a) depicts the obvious

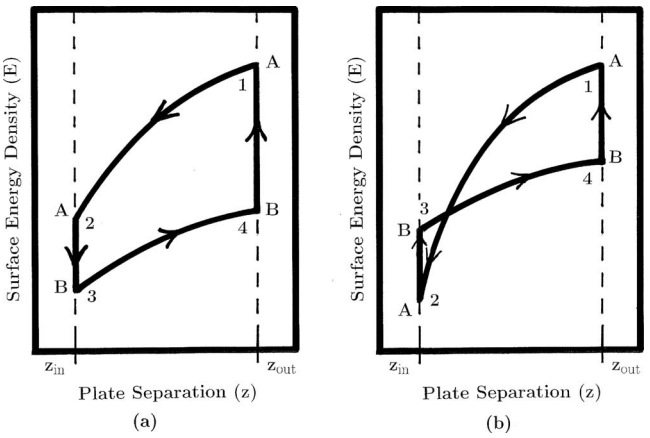

FIG. 3. Variations on Fig. 2: Casimir surface energy density vs plate separation for reaction A⇌B. (a) Converse of energy density vs plate separation relationship in Fig. 2. (b) Inversion of surface energy density with z_{in} and z_{out}.

converse situation: the greater ΔE_{chem} now occurs at z_{in} rather than at z_{out}. Again, thermodynamic steps 1–4 above apply.

For the exothermic reaction A⇌B in Figs. 2 and 3(a), B is energetically favored over A as a product, regardless of z. In principle, however, Casimir interaction energies can be sufficiently strong to invert this order. In Fig. 3(b), as before, substance B is energetically preferred over substance A at z_{out}. Now, however, owing to the large and disproportionate Casimir interaction energy of A versus B, at z_{in} substance A is energetically preferred over B. The crossover point (z_{cross}), where A and B are energetically equal, is given approximately by $z_{cross} \simeq \sqrt{(1/12\pi)|[(H_A - H_B)/(E_A(z_{out}) - E_B(z_{out}))]|}$, where Eq. (1) has been used with zero-separation values for H.

Insofar as the energetic stability translates to thermodynamic stability, a Casimir-induced change in ΔE_{chem} should be reflected as a change in a reaction's chemical equilibrium constant K_{eq}. [For the remaining discussion, "energetically more stable (preferred)" will be taken to be roughly equivalent to "thermodynamically more stable (preferred)."] For the reaction A⇌B, one has $K_{eq} \equiv [B]/[A] = \exp[-\Delta G/RT]$, where ΔG is the molar Gibbs energy and R the gas constant. Although E_{chem} is clearly not G, it can act as a rough proxy, ignoring entropic effects. If so, it may be possible to vary ΔG through $\Delta E_{chemical} = E_2 - E_4$ so as to *tune* the equilibrium ratio of products and reactants for a given reaction at the nanoscale through proper choice of substrates and geometries. In this sense, the equilibrium *constant* becomes a *variable*. (Of course, the usual notion of equilibrium constant can be retrieved by including plate separation and Casimir interaction energy as part of the formal physical specification of the system's state. Here it is left out to highlight the novel role played by the Casimir effect.)

Figures 2 and 3 indicate that reaction energy ΔE_{chem} and the equilibrium constant K_{eq} can be tuned by the Casimir interaction, but they are silent about either the activation energy or chemical pathway for a given reaction. It is likely that these too should be affected by Casimir interactions.

Consider a slice of a hypothetical potential energy landscape [Fig. 4(a)], with energy plotted versus reaction coordinate q. Here case (i) refers to a fiduciary case where no Casimir forces act. As expected for an exothermic reaction A⇌B, A can proceed over the activation energy barrier E_{act}, releasing energy $E_A - E_B \equiv \Delta E_{chem}$. On the other hand, if the reaction energy ΔE_{chem} is increased, holding the reaction coordinate fixed [Fig. 4(a), case (ii)], the canonical force on the system ($F_q \equiv -\partial E/\partial q$) is commensurately increased. Subjected to this greater force, the system should respond to diminish it. As shown in case (ii) of Fig. 4(b), this reduction can be accomplished either by stretching the reaction coordinate between reactant and product or by reducing the activation energy. Both changes lessen the energy gradient, i.e., the canonical force, on the system. Changes in E_{act} are significant since they can exponentially affect reaction rates through the Ahhrenius relation.

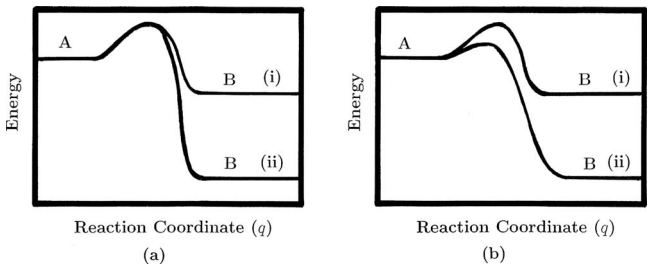

FIG. 4. Chemical energy vs reaction coordinate q for reaction A⇌B. (a) Comparison between no-Casimir interaction case (i) and Casimir interaction case (ii). Greater canonical force indicated for case (ii). (b) System accommodation to Casimir interaction for exothermic reaction: extension in q and reduction in E_{act}.

Additionally, it is conceivable that the Casimir interaction energy could alter chemical pathways, for instance, by changing the relative energetic stabilities between possible reaction products, as suggested in Fig. 5 for the reactions A→B versus A→C. Here, at z_{out}, substance A might pref-

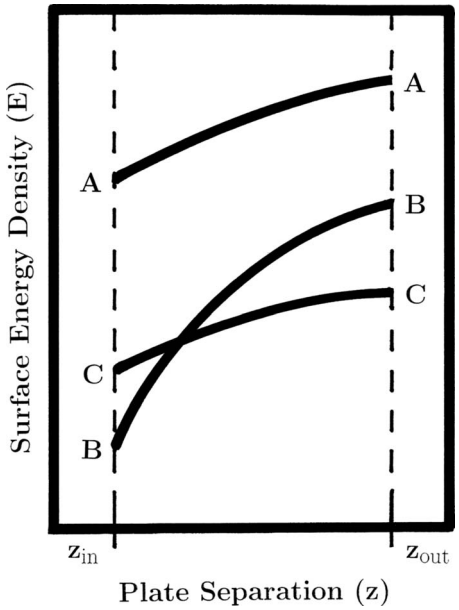

FIG. 5. Redirection of chemical pathway due to Casimir interaction. At z_{out} species C is thermodynamically most favored, while at z_{in} species B is most favored.

erentially convert to C rather than into B owing to the former's greater energetic stability, whereas at z_{in} the situation might be reversed since B is now energetically favored over C.

The Hammond–Leffler hypothesis[28,29] supports these conclusions, positing that the transition state for a reaction should resemble the species nearest to it in energy. With Casimir interactions, where relative energies between products and reactants can be appreciably shifted [or even reversed, as in Fig. 3(b)], the transition state should likewise be shifted to resemble more its energetically nearest species. Furthermore, if the transition state is altered, so too might the pathway through the reaction's potential energy landscape. It follows that the activation energy and reaction rate should likewise be affected.

In summary, it appears likely that Casimir interactions cannot only directly affect energies and chemical equilibria of surface reactions, but also, via the Hammond–Leffler hypothesis, could also affect reaction pathways, activation energies, and reaction rates.

B. Effect magnitude

The magnitude of the Casimir chemical effect can be estimated based on realistic physical parameters. Referring to Fig. 1(b), let substance A have layer thickness $t_A=1$ nm, and at $z_{in}=0.5$ nm let Hamaker coefficients be $H_{\beta m/Am}(z_{in}=0.5\ \text{nm})=H_{\beta m/\alpha A}(z_{in}=0.5\ \text{nm})\simeq 250$ zJ, which are appropriate to substance A being electrically conductive.[30] Again let medium m be vacuum. Let substance B, into which A can convert ($A\rightleftharpoons B$), have Hamaker coefficients $H_{\beta m/Bm}(z_{in}+t_A)=H_{\beta m/\alpha B}(z_{in}+t_A)\simeq 50$ zJ, appropriate if B is nonconducting. Given these parameters, the difference in surface reaction energy density ΔE_{chem} between plate separations z_{in} and z_{out} can be shown to be roughly $\Delta E_{Cas}\equiv|\Delta E_{chem}(z_{out})-\Delta E_{chem}(z_{in})|\simeq 2\times 10^{-2}$ J/m^2. The maximum Casimir interaction energy densities are about two orders of magnitude less than the energy densities necessary to reform all chemical bonds on a surface. (This assumes 2 bonds/atom, 5 eV/bond, and 10^{19} atoms/m^2.) This suggests that this effect should be most important either for reactions in which reactants and products are nearly energetically degenerate or for reactions of relatively large molecules having specifically targetable reaction channels.

The physical manifestation of this Casimir chemical energy should depend critically on the surface areal footprints (m^2) of the participating molecules. (Let other physical properties of A and B be identical (e.g., mass density, bulk modulus), so as not to otherwise affect the energetics.) Let $S_A=S_B\equiv S$ be the areal footprints of A and B and let η be the average ΔE_{Cas} per molecule. In Fig. 6 is plotted $\log(\eta)$ versus $\log(S)$. In order to interpret this plot quantitatively, Table II presents several benchmark energies and energy scales. For reference, energy benchmarks are included in Fig. 6, as well as characteristic size scales for molecular classes.

Several observations can be made. Taking the surface footprint of an atom or small molecule on a surface to be roughly 10^{-19} m^2, Eq. (5) predicts the maximum Casimir

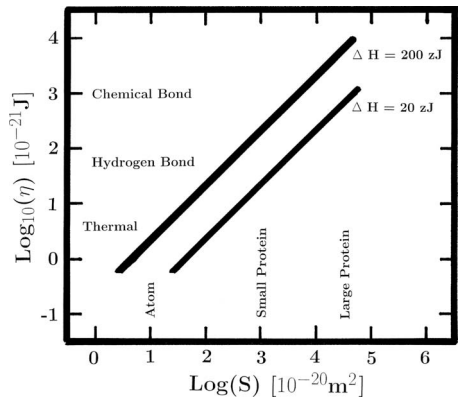

FIG. 6. Casimir energy per molecule (η) vs molecular areal footprint (S) for $\Delta H=200$ zJ and $\Delta H=20$ zJ. Energy benchmarks and characteristic molecular sizes are labeled.

interaction energy to be roughly 2 zJ or roughly $\frac{1}{2}kT$ at temperature $T=300$ K. This is thermally appreciable and enough to perhaps drive conformational changes (e.g., a *gauche* to *anti* conformation in a sterically hindered organic molecule), but little else. (Or, if the A-layer is freestanding rather than deposited on the α-plate, then this $\frac{1}{2}kT$ might be manifested as thermal energy, locally heating the sample.) For larger molecules, with footprints on the order of 30–50 atoms ($\sim 3\times 10^{-18}$ m^2), the Casimir energy can be 80 zJ, roughly $20kT$, comparable to that of a hydrogen bond. Still larger molecules, such as typical proteins ($S\sim 10^{-17}-10^{-16}$ m^2), the Casimir energy can be comparable to that of one to perhaps several chemical bonds. (Of course, if the excess Casimir interaction energy was not uniformly distributed over the surface, but instead concentrated in spots, then in principle, energy densities sufficient for chemical bonds might be attained even for small molecules.)

Casimir energy can be understood in terms of pressure-volume work. Just as gas pressure can provide the energy for bulk chemical transformations, so too can Casimir pressure. The magnitude of the Casimir pressure between suitable dielectrics can be inferred from Eq. (1) to be $\mathcal{P}=-\partial E/\partial z=-H/6\pi z^3$. Across pure vacuum at a plate separation of $z=2$ nm, this pressure can exceed 100 atms. This Casimir surface energy density is comparable to that of pressure-volume surface work density for a displacement of 100 nm under 1 atm of pressure.

In standard gas pressure-volume work scenarios, pressure differentials are understood at the microscopic level as due to differential momentum flux densities from gas molecules. As shown by Milonni *et al.*,[31,3] Casimir pressure can be understood analogously as due to the differential momen-

TABLE II. Benchmark energies for representative physical chemical phenomena in various energy units.

Energy type	kT	zJ	eV	kcal/mole
Thermal (300 K)	1	4	0.026	0.5
Conformational	2	8	0.05	1
Physisorption	2	8	0.05	1
Hydrogen bond	20	80	0.5	10
Chemical bond	200	800	5	100

tum flux densities of virtual photons between the interior and exterior surfaces of closely spaced plates. As such, Casimir pressure-volume work is not mysterious; rather, it is the expected outcome of virtual photons whose mode densities have been constrained by the boundary conditions imposed by the confining dielectric plates.

How Casimir interaction energy is expressed—as conformational changes, chemical bonds, changes in bulk physical properties, or simply as excess heat—should depend on the reaction channels available in the system. Molecules exhibiting robust zero point effects are likely to have relatively large areal footprints since Casimir energy scales linearly with area, but they should also be relatively flat since the majority of this energy will be distributed within about a wavelength of the substrate's surface. Second, because Casimir-induced changes in energy are derived from changes in the relative differences in dielectric susceptibilities [Eq. (3)], it would seem to be advantageous that the dielectric responses be distributed over large distances in the candidate molecules, perhaps via delocalized electrons. This suggests that highly conjugated or aromatic organics or polymers might be good Casimir candidates, such as derivatives of polyacetylene, polyaniline, polypyrrole, or polyphenylene. Additionally, it would seem advantageous that small changes in molecular structure give rise to large changes in susceptibility, as seen in the electronic behavior of molecular resonant tunneling diodes[32] or in shape-sensitive biomolecules such as proteins.[33,34] Detailed consideration of Casimir chemical candidates is beyond the scope of this paper.

It is emphasized that Casimir chemical effects are not due to standard surface chemical potentials; they are distinct in at least two important ways. First, surface potentials involve quantum and Coulombic interactions among surface atoms and electrons, whereas Casimir effects are attributable to virtual electromagnetic modes of the vacuum interacting with the bulk medium. Second, compared with usual chemical surface potentials,[35] Casimir effects are long range. They should to be manifest out to the long wavelength limit of the Casimir force, roughly a few microns, which is two to three orders of magnitude greater than the typical range of surface chemical potentials. Admittedly though, the most dramatic Casimir effects operate out to only a few nanometers, less than an order of magnitude greater distance than standard surface potentials. In this respect, Casimir energy can be taken as secondary to surface potential, especially given the larger energies typically associated with the latter.

IV. APPLICATIONS

Casimir chemical energy effects could be expressed through a variety of applications. Here we briefly consider a few possibilities.

A. Casimir Catalysts

Catalysts form the backbone of the world's chemical industry, contributing to the manufacture of roughly 90% of commercial chemical products. As enzymes, abzymes, and ribozymes, they render life possible. Hallmarks of traditional catalysts are the abilities to lower activation energies, modify transition states and reaction rates, while not being consumed in the reactions. The Casimir systems considered thus far satisfy these criteria; however, they can also apparently change reaction energies and equilibrium constants, setting them apart in fundamental ways. For this discussion they will be called *Casimir catalysts*.

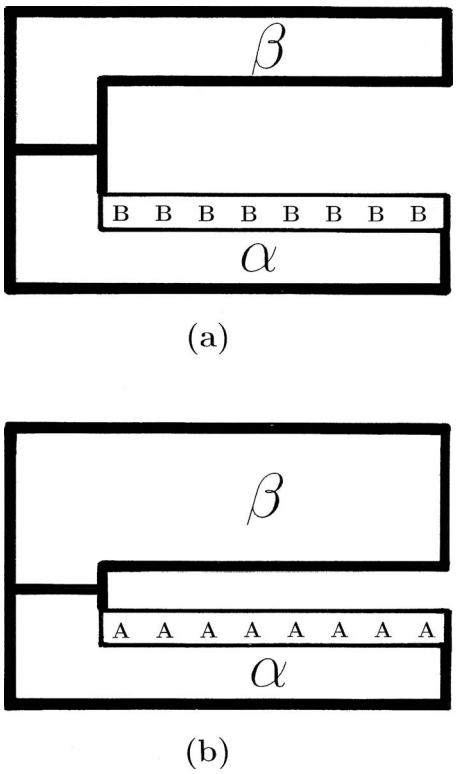

FIG. 7. Casimir catalysts. (a) Nanocatalyst particle with large plate separation: species B preferred. (b) Nanocatalyst particle with small plate separation: species A preferred.

On a purely academic level, it might be argued that Casimir catalysts are not possible because they shift chemical equilibria, whereas it is normally understood that a catalytic shifting of equilibrium can lead to a violation of the second law of thermodynamics. This objection is not valid here because any exess in chemical energy resulting from a Casimir cycle (e.g., Figs. 2 and 3) can be traced to net work performed against Casimir force, not supplied by a heat bath; thus, the second law is not challenged.

One can envision tuning the size and structure and composition of Casimir catalysts to optimize the output of a particular product or intermediate in a reaction or to suppress unwanted side products. Figures 7(a) and 7(b) depict two possible structures. [Figure 3(b) gives the energy density–gap width diagram pertaining to them.] The catalyst particle in Fig. 7(a) has a relatively wide gap such that substance B is energetically (thermodynamically) favored over substance A, whereas in the case of a narrow gap [Fig. 7(b)], substance A is favored over substance B. In principle, both A and B could be present side by side if, for instance, one inner surface of the catalyst particle was corrugated.

This physical situation can be complicated by electrostatic potentials between the plate materials owing to differences in their chemical potentials. (For semiconductors these

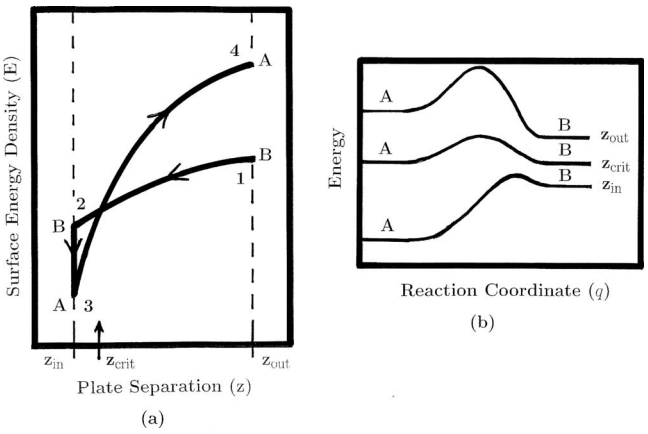

FIG. 8. Zero point molecular forge. (a) Casimir surface energy density vs plate separation for reaction A⇌B. (b) Chemical energy vs reaction coordinate for various plate separations. Activation energy barrier decreases with decreasing z.

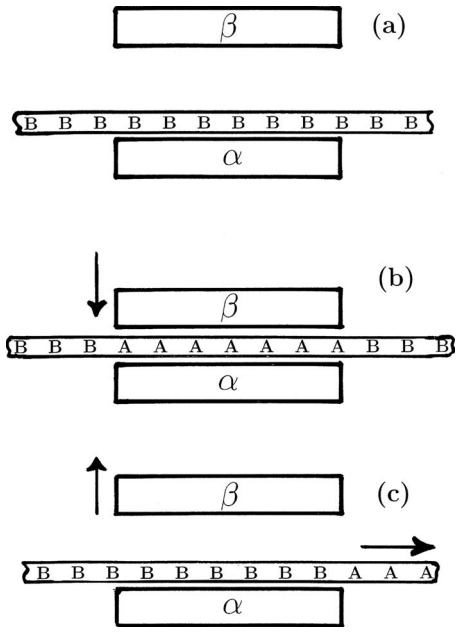

FIG. 9. Operation of zero point molecular forge. (a) Ribbon B in gap with β-plate retracted out to z_{out}. (b) β-plate at z_{in} forging B into A. (c) β-plate retracting, forged A pulled out, and new charge of B inserted.

are called *built-in* potentials, while for metals they are *contact* potentials.) These would be expressed at the α-β material interface and also across the vacuum gap where they could appear as large electric fields. Such *intrinsically biased electrocapacitive catalytic* effects have been discussed elsewhere.[36] Here they can be simply avoided by creating the nanocatalyst particles out of a single material, say β. The zero point effects would remain, subject to their redefinition with $\alpha=\beta$ in Eqs. (1)–(5).

In summary, static arrangements of nanoscopically spaced plates should favor particular molecular species, allowing new types of nanocatalysts.

B. Casimir molecular forge

The idea of Casimir catalyst can be extended to the dynamic case. Because the thermodynamic stability of chemical species can depend on plate separation z, it should be possible to convert one chemical species into another (e.g., A into B) simply by moving the Casimir reaction plates with respect to each other. This dynamic process will be called *Casimir molecular forging*.

To concretize these ideas, consider the thermodynamic cycle in Fig. 8(a), the reverse of the cycle in Fig. 3(b). At z_{out} species B is thermodynamically favored, while at z_{in} the reverse is true. Figure 8(b) plots chemical energy versus reaction coordinate q. The activation energies at z_{out} and z_{crit} are sufficiently high that the thermally driven reaction rate is negligible on the timescale of the forge's mechanical motion, while at z_{in} the activation energy is sufficiently low that it can easily be surmounted thermally on these timescales. (Recall from Sec. III A that Casimir interactions can affect both activation energy and reaction rates.)

Figure 9 depicts a molecular forge in various stages of operation. Let the β-plate begin at z_{out} and let A and B be at thermodynamic equilibrium; i.e., B is in excess over A. As the plates are brought together, the energy of A decreases more rapidly than B and, furthermore, the activation energy barrier falls. By the time the plate reaches z_{in}, species B has thermally converted largely into A. Now, as the plate is returned to z_{out}, species A is unable to thermally surmount its activation energy barrier back to B. The net result of the cycle is to convert (forge) low-energy B into high-energy A. Of course, to satisfy energy conservation, this net increase in chemical energy is supplied by the net mechanical work done against the Casimir force. (Notice that Step 1→2 provides less work output than Step 3→4 requires.)

This Casimir work can be likened to standard pressure-volume work that might be performed to forge, say, a low-energy elemental form of carbon (graphite) into a higher-energy metastable form (diamond). In the present case (B→A), however, the forge pressure is distinct in two ways: (a) its sign is usually negative owing to the typically attractive nature of the Casimir force; and (b) it is not conveyed by a material substance (gas, fluid, solid, or even real photons), but rather by virtual photons of the quantum vacuum. Thus, this zero point process offers another way to drive chemical reactions without necessitating material intermediates to transmit pressure. Classical electromagnetic analogs would be the pressures exerted on free charges and currents by electric and magnetic fields.

Let us examine the molecular forge more systematically. In Fig. 9(a), the chemical-mechanical cycle begins with a ribbon of species B pulled into place between the stationary α-plate and the movable β-plate. (In principle, the α-plate is unnecessary since the B-ribbon can be freestanding.) In Fig. 9(b), the β-plate is brought down toward the ribbon, this corresponding to Step 1→2 in Fig. 8(a). At z_{in}, species B thermally converts into species A [Step 2→3 in Fig. 8(a), based on the energetics shown in Fig. 8(b)]. Finally, in Fig. 9(c), the β-plate is retracted against the increased Casimir force [Step 3→4, Fig. 8(a)], and the ribbon is pulled out from between the plates, after which a new charge of B is brought into the gap to complete the cycle. As the net result, a length of ribbon B has been chemically forged into species

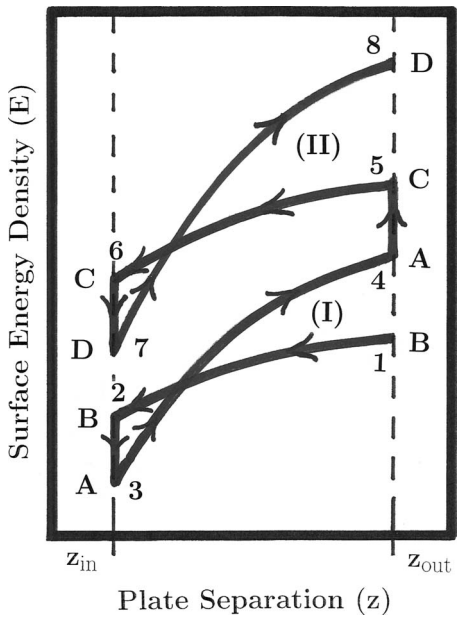

FIG. 10. Casimir two-cycle: surface energy density vs plate separation for net reaction B→D. Cycle I (Steps 1→4 for reaction B→A) connected to cycle II (Steps 5→8 for reaction C→D) by bridging reaction (Step 4→5 for reaction A→C).

A. Again, note that Casimir forging does not require direct contact between the reacting ribbon and either plate α or β.

In summary, it seems possible to nanomechanically forge chemicals via a work cycle involving the Casimir force, where zero point fluctuations act as the working fluid. This represents a novel nanoscale technique to convert mechanical energy directly into chemical energy. The current art of micro- and nanoelectromechanical systems (MEMS and NEMS) appears adequate to allow tests of this concept.[37,38] Perhaps such "virtual" chemical processes will become commonplace in future nanoscale chemistry.

C. Casimir multicycles

It appears possible to use multiple, interlinked Casimir cycles to *bootstrap* upward in energy, beyond the limitations of a single cycle. Consider the multistep chemical pathway depicted in Fig. 10, whereby B is converted through two Casimir cycles into high-energy product D (B→A→C→D). Two independent cycles (I and II) are linked by a bridging reaction A→C, perhaps driven by an external reactant. The total chemical energy increase over the two-cycle consists of the energy of the bridging reaction ΔE_{bridge} plus those of the two Casimir cycles $\Delta E_{\text{I,II}}$, namely, $\Delta E_{\text{chem,total}} = \Delta E_{\text{I}} + \Delta E_{\text{II}} + \Delta E_{\text{bridge}}$. As before, the chemical energies $\Delta E_{\text{I,II}}$ are provided by net mechanical work against the Casimir force performed by the β-plate.

An even more streamlined version of this bootstrap process can be imagined (Fig. 11). Here, the reaction A→B→D is carried out via two Casimir cycles without recourse to a bridging reaction [Fig. 11(a)]. Here the reaction plate is double-sided [Fig. 11(b)]. Plate-β is used for cycle I, then flipped over at Step 4 to expose plate-γ for cycle II. (Clearly, this requires that the Casimir interaction energy of species A with plate media β and γ be suitably disparate.) The net

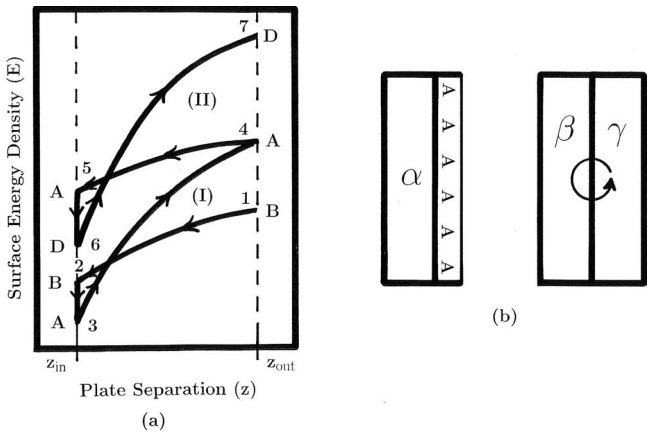

FIG. 11. Streamlined Casimir two-cycle: surface energy density vs plate separation for net reaction B→D. (See Fig. 10.) (a) Energy bridging reaction (A→C) absent. (b) Rotatable dual surface (β/γ) movable plate for molecular forge, pertinent to (a).

chemical energy change for this double cycle is $\Delta E_{\text{chem,total}} = \Delta E_{\text{I}} + \Delta E_{\text{II}}$. In principle, an arbitrary number of Casimir cycles can be linked to build up chemical energy. The maximum energy gain, however, is limited ultimately by differences in dielectric susceptibilities between interacting materials.

D. Casimir chemical engines

Chemically driven nanoscopic machines and motors (engines) take many of forms. The first, most efficient, and most complex molecular machines are biological, e.g., actin-myosin, kinesin, and flagellar motors, powered by adenosine triphosphate (ATP).[33,34] Manmade molecular machines—motors, rotors, ratchets, shuttles, switches, and tweezers—have been synthesized to be powered by electric currents, gradients in temperature and chemical potentials, light, or other reactive molecules.[37] NEMS are solid-state devices powered almost exclusively by electric fields.[38,39] Their chemical powering is indirect, via batteries or fuel cells. Casimir effects might offer an additional route to direct chemical drive at the nanoscale. Additionally, it does not require direct physical contact between a device's moving parts, a leading cause of damage and failure in standard NEMS and MEMS.

Just as an electric motor run in reverse acts as an electrical generator, so too should the Casimir molecular forge (Sec. IV B) run in reverse act as a molecular motor, transforming chemical energy into mechanical motion. Again zero point radiation acts as the working fluid in a thermodynamic cycle. A traditional thermodynamic analog would be a steam engine driven by chemical reactions (burning coal), with steam as the working fluid, operating between hot and cold heat reservoirs. Here the hot and cold reservoirs are replaced by UV (hot) and IR (cold) vacuum fluctuations that predominate at z_{in} and z_{out}, respectively. Purely photonic heat engines have been examined by others;[40,41] some incorporate zero point fluctuations.[42] The present proposal is unique in linking chemical changes to changes in the zero point field.

Consider Fig. 12, a modified version of the dielectric plates in Fig. 1(b). The stationary α-plate is unchanged,

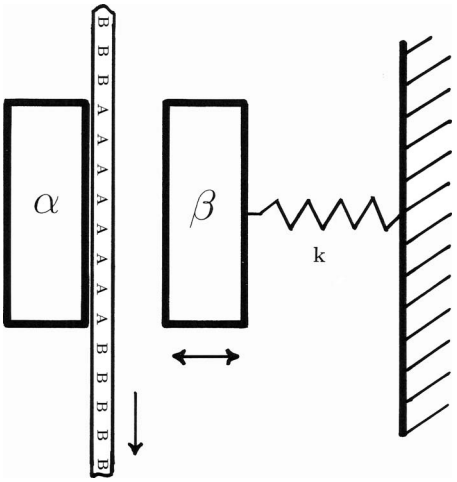

FIG. 12. Mechanically driven zero point engine with alternating A-B ribbon drive. β-plate oscillation energy provided by forcibly pulling ribbon through gap. [For self-propelling ribbon, the upper precursor section (B-ribbon) must be pure A-ribbon.]

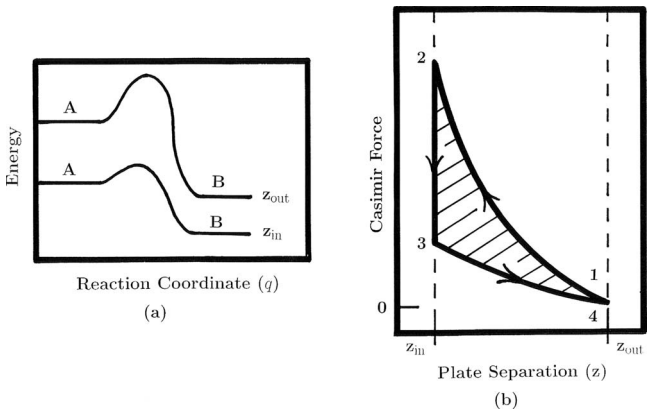

FIG. 13. Zero point engine. (a) Chemical energy vs reaction coordinate at z_{out} and z_{in} pertinent to cycle in Fig. 2. (b) Traditional thermodynamic *P-V* work cycle: Casimir force vs plate separation. Area enclosed by cycle is ideal work output. β-plate oscillation energy provided by ΔE_{Cas}.

while the movable β-plate (mass m_β) is attached to a spring (spring constant k_s) and acts as a piston. The surface layer of substance A is replaced by a long, flat translatable ribbon extending beyond the gap, consisting of alternating sections of substances A and B, having different Hamaker coefficients. For the moment, A and B are unable to chemically interconvert.

Let the Casimir interaction diagram for A and B be the same as in Fig. 2, where A exhibits stronger Casimir interactions than B. It is easy to show that, if the ribbon is forcibly pulled through the gap at a linear rate commensurate with the natural mechanical oscillation frequency of the β-plate, a resonant oscillation of the piston can be excited, with frequency $\omega_{res}=\sqrt{k_s/m_\beta}$. The mechanical energy for the oscillation derives from the work necessary to pull the ribbon through the gap against the restoring Casimir force. Like the oscillation of a child's swing, pumped by leg and arm motion, the forced synchronous insertion of low- and high-Hamaker sections of ribbon into the gap pull and release the piston, subject to the restoring force of the spring. Specifically, high-Hamaker substance A moves through the gap during the instroke, pulling the β-plate piston to the left and stretching the spring, while low-Hamaker substance B moves through during the outstroke, releasing the piston and allowing the spring to retract it.

This oscillation can be driven purely chemically—as apposed to mechanically by forcibly pulling the ribbon—if the reaction $(A \rightarrow B)$ is allowed to proceed. In this case, let a ribbon of pure A move through the gap subject to the Casimir cycle in Fig. 2 and the reaction energy diagram in Fig. 13(a).

As before in Fig. 8(b), at z_{out} the activation energy barrier cannot be surmounted thermally on the timescale of the piston's motion $(\tau \sim \sqrt{m_\beta/k_s})$, whereas at z_{in} the barrier is low enough to be quickly surmounted thermally. Beginning at point 1 in Fig. 2, with the piston moving inwardly and the spring unstretched, the Casimir engine cycle proceeds as follows.

Step $1 \rightarrow 2$: With A in the gap, the piston is pulled inwardly (to the left) by the Casimir force, stretching the spring. Substance A remains stable against thermal conversion into B by a high activation energy barrier.

Step $2 \rightarrow 3$: At z_{in} the activation energy barrier is lower so that the reaction $A \rightarrow B$ proceeds rapidly.[43] Substance B's smaller, attractive Casimir force is overcome by the retracting force of the spring, accelerating the piston outwardly (to the right).

Step $3 \rightarrow 4$: The piston moves from z_{in} to z_{out}, relaxing the spring, and overshooting its equilibrium position.

Step $4 \rightarrow 1$: The newly created B-section of the ribbon is forced out of the gap by a new section of A that replaces it.[44] The piston returns to its initial configuration, and the cycle repeats.

This cycle can be recast as a standard thermodynamic engine work cycle. In Fig. 13(b) is plotted the Casimir force $(F_{Casimir} \equiv -\partial E/\partial z)$ versus gap width z. The cycle proceeds as above in Fig. 2. The area enclosed by the cycle is the work performed in an ideal cycle. Note that this cycle is essentially the reverse of the Casimir molecular forge of Sec. IV B.

The power of an individual Casimir engine should be tiny, but its power density could be substantial. Taking the surface energy density of the piston plate to be $\rho_E \sim 10^{-2}$ J/m^2 and its operating frequency to be typical of radio frequency NEMS $(f \sim 10^9$ Hz), its power density would be appreciable: $P \equiv \rho f \simeq 10^7$ W/m^2.

In summary, Casimir effects might be used to help drive nanoscopic chemical-mechanical engines. They are currently under active study and will be reported upon in greater depth in future communications.

E. Casimir biochemistry

Life can be described as a complex, autocatalytic network of chemical reactions guided by nanoscopic molecular machines.[45,33,34] Casimir chemical effects could conceivably play a role in some of these machines.

Insofar as many of the micro- and nanoscopic structures naturally present in cells seem conducive to the Casimir effect (e.g., biplanar cell membranes, spherical vesicles, cylindrical microtubules[46]); and inasmuch as many biochemical reactions turn on energetic changes comparable to those pre-

dicted for Casimir chemistry (e.g., conformational and steric effects, hydrogen bonding); and since Life seems compelled to exploit any possible process in service of natural selection, it is predicted that Casimir chemistry will be discovered at the cellular level, most likely in the context of reactions on the boundaries of some of the above cellular structures. Indeed, some of the most consequential processes in biochemistry—e.g., protein folding, DNA coiling, drug binding—rely on some of the weakest and most subtle forces, including ones already directly linked to vacuum fluctuations, e.g., van der Waals forces. Perhaps this is not surprising; after all, subtlety and sensitivity hold sharp the razor's edge between order and chaos, upon which Life must tread.

V. FUTURE DIRECTIONS

In this paper, ideas for Casimir chemistry have been sketched in broad strokes, overlooking many details. At the most basic level, the effects of intervening dielectric other than vacuum have not been pursued, although many, if not most, real industrial and biological processes are likely to involve water or other solvents. Thus far, only negative pressure Casimir effects have been addressed, whereas both theory and experiment confirm that positive (repulsive) Casimir effects are also possible[26,47,48] and could give rise to novel applications, like push-pull motors. Furthermore, only parallel plate geometry has been considered, although other geometries (e.g., spherical, cylindrical, elliptical, corrugated) are likely to be pertinent elsewhere. The many possible interactions and feedbacks between Casimir energy and surface chemical or electrostatic potentials should also be explored.

Because the maximum Casimir interaction energy densities are relatively low ($\sim 10^{-2}$ J/m^2), channeling this energy into high-energy reactions would seem to require specialized molecules and reaction channels that "focus" this energy and preclude its loss via perhaps more ubiquitous low-energy routes, e.g., multiple low-energy conformational rearrangements rather than a single chemical bond. Among the many candidate classes of molecules, highly conjugated or aromatic electrically conducting or diodic organic polymers stand out since they are likely to have relatively large Hamaker coefficients and large, flat surface footprints. Molecules whose chemical activities turn on small changes in structures or energies, e.g., proteins and other biomolecules, should also be considered. Regardless, at this time it seems likely that Casimir chemical effects can be important only for limited classes of molecules.

It would be significant if a way was discovered to intensify zero point energy densities inside reaction volumes so as to increase the energy available for reactions. Even small improvements in energy densities would likely exponentially increase the number and type of candidate reactions. Some claims have been made along these lines, e.g., the dynamic Casimir effect as applied to sonoluminescence,[49] but these do not enjoy consensus support.[50] Whether specialized geometries, materials, or constructions (e.g., metamaterials) can locally intensify zero point fields remains an open question.

From a broader perspective, perhaps it should not be surprising that the Casimir force should have chemical ramifications. After all, it is intimately related to the van der Waals force, which has deep connections in chemistry. The van der Waals interaction is a principal long-range "bond" between gas molecules, and it can be key in liquids, as evidenced by surface tension. It bears strongly on the melting points of nonpolar solids (e.g., paraffin) and, as noted above, it can be paramount to sensitive biochemical reactions. Still, the Casimir effect's chemical implications appear not to have been examined carefully before, and deeper exploration might reveal new applications as well as theoretical research directions.

In summary, a new chemical effect is proposed based on the Casimir effect whereby fundamental aspects of chemical reactions—e.g., reaction energy, equilibrium constants, activation energies, and reaction pathways—can be tuned. These Casimir chemical effects might inspire new applications, including nanocatalysts, Casimir molecular forges, and engines. It is speculated that these zero point effects might already operate in cellular processes.

ACKNOWLEDGMENTS

The author is grateful to Dr. T. Herrinton, Dr. P. Greene, Dr. E. J. Page, Dr. J. P. Sullivan, Dr. D. C. Cole, and Dr. P. W. Milonni for illuminating conversations, and to C. L. Proctor, J. K. Ramis, and S. H. Nogami for the initial impetus to explore this subject. The author also thanks the anonymous reviewer for helpful suggestions. This work was conducted with the support of a University of San Diego faculty reassign time award (2008). This work was performed in part at the Center for Integrated Nanotechnologies, Office of Basic Energy Sciences user facility, at Los Alamos National Laboratory (Contract No. DE-AC52-06NA25396) and Sandia National Laboratories (Contract No. DE-AC04-94AL85000). This work is dedicated to the memories of Dr. William F. Sheehan and Patrick C. Sheehan.

[1] M. Planck, Ann. Phys. **37**, 642 (1912).
[2] A. Einstein, Ann. Phys. **40**, 551 (1913).
[3] P. W. Milonni, *The Quantum Vacuum: An Introduction to Quantum Electrodynamics* (Academic, Boston, 1994).
[4] H. B. G. Casimir, Proc. K. Ned. Akad. Wet. **51**, 793 (1948).
[5] A. Einstein, Phys. Z. **18**, 121 (1917).
[6] P. C. W. Davies, J. Phys. A **8**, 609 (1975).
[7] W. G. Unruh, Phys. Rev. D **14**, 870 (1976).
[8] W. E. Lamb and R. C. Retherford, Phys. Rev. **72**, 241 (1947).
[9] H. A. Bethe, Phys. Rev. **72**, 339 (1947).
[10] H. B. G. Casimir and D. Polder, Phys. Rev. **73**, 360 (1948).
[11] F. London, Z. Phys. **63**, 245 (1930).
[12] D. Langbein, *Theory of Van der Waals Attraction*, Springer Tracts in Modern Physics Vol. 72 (Springer-Verlag, Berlin, 1974).
[13] V. A. Parsegian, *Van der Waals Forces: A Handbook for Biologists, Chemists, Engineers, and Physicists* (Cambridge University Press, Cambridge, 2006).
[14] P. Kusch and H. M. Foley, Phys. Rev. **74**, 250 (1948).
[15] D. C. Cole and Y. Zou, Phys. Lett. A **317**, 14 (2003).
[16] J. Schwinger, L. L. DeRaad, Jr., and K. A. Milton, Ann. Phys. (N.Y.) **115**, 1 (1978).
[17] P. W. Milonni and P. B. Lerner, Phys. Rev. A **46**, 1185 (1992).
[18] E. J. Kelsey and L. Spruch, Phys. Rev. A **18**, 15 (1978).
[19] F. Pinto, Phys. Rev. B **60**, 14740 (1999).
[20] E. M. Lifshitz, Sov. Phys. JETP **2**, 73 (1956).

[21] E. E. Dzyaloshinskii, E. M. Lifshitz, and L. P. Pitaevskii, Adv. Phys. **10**, 165 (1961).
[22] B. V. Darjaguin, I. I. Abrikosova, and E. M. Lifshitz, Q. Rev., Chem. Soc. **10**, 295 (1956).
[23] S. K. Lamoreaux, Phys. Rev. Lett. **78**, 5 (1997).
[24] J. N. Munday and F. Capasso, Phys. Rev. A **75**, 060102(R) (2007).
[25] G. Bressi, G. Carugno, R. Onofrio, and G. Ruoso, Phys. Rev. Lett. **88**, 041804 (2002).
[26] Similar behavior is expected for more complex geometries subject to their particular force laws. Surface shape and curvature can affect not only the magnitude of the effect but also its character—attractive or repulsive [T. H. Boyer, Phys. Rev. **174**, 1764 (1968)]. In general, however, when structures are near enough that their local radii of curvatures are large compared with their separations, the parallel plate approximation holds.
[27] Equation (2) assumes that (a) the differences in ϵ are small, (b) magnetic susceptibilities are negligible, and (c) the speed of light in media α and β is the same as in medium m. Although not exact, Eq. (2) captures the essential features of the parallel plate system. The $'$ in the sum refers to taking $1/2$ of the $n=0$ term.
[28] G. S. Hammond, J. Am. Chem. Soc. **77**, 334 (1955).
[29] J. E. Leffler, Science **117**, 340 (1952).
[30] This layer thickness of A (1 nm) is chosen to roughly match optimal plate separation since the Casimir forces should operate down into the surface of A roughly this distance and 0.5 nm is the rough lower limit where the continuum approximation can hold for Eqs. (1)–(5).
[31] P. W. Milonni, R. J. Cook, and M. E. Goggin, Phys. Rev. A **38**, 1621 (1988).
[32] J. C. Ellenbogen and J. C. Love, in *Handbook of Nanoscience, Engineering, and Technology*, edited by W. A. Goddard III, D. W. Brenner, S. E. Lyshevski, and G. J. Iafrate (CRC, Boca Raton, 2003), pp. 7.1–7.64.
[33] P. Nelson, *Biological Physics: Energy, Information, Life* (Freeman, New York, 2004).
[34] M. Kurzynski, *The Thermodynamic Machinery of Life* (Springer-Verlag, Berlin, 2006).
[35] R. I. Masel, *Principles of Adsorption and Reaction on Solid Surfaces* (Wiley, New York, 1996).
[36] D. P. Sheehan and T. Seideman, J. Chem. Phys. **122**, 204713 (2005).
[37] Unfortunately for us, man-made machines are to biological machines in complexity and ingenuity as the yo-yo is to the eight-speed automatic transmission.
[38] *Micromechanics and MEMS: Classic and Seminal Papers to 1990*, edited by W. Trimmer (IEEE, New York, 1997).
[39] J. A. Pelesko and D. H. Bernstein, *Modeling MEMS and NEMS* (Chapman and Hall, London/CRC, Boca Raton, 2003).
[40] A. Bartoli, Nuovo Cimento **15**, 193 (1884).
[41] M. H. Lee, Am. J. Phys. **69**, 874 (2001).
[42] J. J. Mareš, V. Špička, J. Krištofik, and P. Hubik, AIP Conf. Proc. **643**, 273 (2002).
[43] Alternatively, conversion of A into B can be driven by chemical means, e.g., by introducing a reactant (C) into the gap ($A+C \rightarrow B$) when the gap is closed.
[44] It can be shown via the principle of virtual work that, in the absence of friction, the ribbon can be self-propelling through the gap. Once B is created (Step $2 \rightarrow 3$) a lateral Casimir force will arise, owing to the stronger Casimir interaction with A, pulling a new charge of A into the gap, thereby expelling the spent B.
[45] S. A. Kauffman, *The Origins of Order: Self-Organization and Selection in Evolution* (Oxford University Press, New York, 1993).
[46] S. Hameroff, private communications (2009); S. Hagan, S. Hameroff, and J. Tuszynski, Phys. Rev. E **65**, 061901 (2002).
[47] A. Milling, P. Mulvaney, and I. Larson, J. Colloid Interface Sci. **180**, 460 (1996).
[48] J. N. Munday, F. Capasso, and V. A. Parsegian, Nature (London) **457**, 170 (2009).
[49] J. Schwinger, Proc. Natl. Acad. Sci. U.S.A. **93**, 958 (1993).
[50] M. P. Brenner, S. Hilgenfeldt, and D. Lohse, Rev. Mod. Phys. **74**, 425 (2002).